Article:
Chappell, S, Brooke, C, Nichols, RJ et al. (2016) Evidence for a hopping mechanism in metal|single molecule|metal junctions involving conjugated metal–terpyridyl complexes; potential-dependent conductances of complexes $[M(pyterpy)_2]^{2+}$ (M = Co and Fe; pyterpy = 4′-(pyridin-4-yl)-2,2′:6′,2″-terpyridine) in ionic liquid. Faraday Discussions, 193. pp. 113-131. ISSN: 1359-6640

https://doi.org/10.1039/C6FD00080K

Evidence for a hopping mechanism in metal | single molecule | metal junctions involving conjugated metal–terpyridyl complexes; potential-dependent conductances of complexes $[M(pyterpy)_2]^{2+}$ (M = Co and Fe; pyterpy = 4'-(pyridin-4-yl)-2,2':6',2''-terpyridine) in ionic liquid.

Sarah Chappell[1], Carly Brooke[1], Richard J. Nichols[1], Laurence J. Kershaw Cook,[2] Malcolm Halcrow,[2] Jens Ulstrup[3] and Simon J. Higgins[1]*

1. Department of Chemistry, University of Liverpool, Crown Street, Liverpool L69 7ZD, U.K.
2. School of Chemistry, University of Leeds, Leeds LS2 9JT, U.K.
3. Department of Chemistry, Department of Chemistry, Kemitorvet, Technical University of Denmark, DK-2800 Kgs. Lyngby, Denmark.

ABSTRACT

Extensive studies of various families of conjugated molecule in metal | molecule | metal junctions suggest that the mechanism of conductance is usually tunnelling for molecular lengths < ca. 4 nm, and that for longer molecules, coherence is lost as a hopping element becomes more significant.[1-4] In this work we present evidence that, for a family of conjugated, redox-active metal complexes, hopping may be a significant factor for even the shortest molecule studied (ca. 1 nm between contact atoms). The length dependence of conductance for two series of such complexes which differ essentially in the number of conjugated 1,4–C_6H_4– rings in the structures has been studied, and it is found that the junction conductances vary linearly with molecular length, consistent with a hopping mechanism, whereas there is significant deviation from linearity in plots of log(conductance) vs. length that would be characteristic of tunnelling, and the slopes of the log(conductance)–length plots are much smaller than expected for an oligophenyl system. Moreover, the conductances of molecular junctions involving the redox–active molecules, $[M(pyterpy)_2]^{2+/3+}$ (M = Co, Fe) have been studied as a function of electrochemical potential in ionic liquid electrolyte, and the conductance–overpotential relationship is found to fit well the Kuznetsov–Ulstrup relationship, which is essentially a hopping description.

INTRODUCTION

The development of techniques that allow the electrical properties of molecules to be investigated in metal | molecule | metal 2-terminal junctions down to the single–molecule level has stimulated renewed interest in truly 'molecular' electronics in the last decade.[1-3] Early work focused mainly on testing different molecular backbones and metal–molecule contact groups to maximise molecular junction conductance.[4] For molecules that conduct by a tunnelling mechanism, the tunnelling current I_T decays exponentially with molecular length according to the equation $I_T = Ae^{-\beta n}$ where the factor A is largely governed by the nature of the contact, β is called the decay constant and is mainly determined by the nature of the

molecular backbone, and n can be expressed either as the number of repeat units in oligomers of varying length, or simply as the length of the molecule (in which case the units of β are (length)$^{-1}$). Since the Fermi energy of the metal contacts must lie between the HOMO and LUMO levels of the molecule, it follows that in general, the lower the HOMO-LUMO separation, the more slowly does molecular conductance fall with length (the smaller is β). The lowest values of β found for purely organic, non-redox-active molecules so far have been with oligo-carbynes ($\beta = 0.6 \pm 0.3$ nm^{-1}).[5] For some conjugated redox-active molecules, such as 'fused-tape' oligoporphyrins (0.19 ± 0.01 nm^{-1})[6] and oligoviologens (0.06 ± 0.004 nm^{-1}),[7] even lower values have been found, but in some of these cases, it is difficult to distinguish between an exponential decay of conductance with length involving a very low β (tunnelling), and a linear decay with length expected for a 'hopping' mechanism.

There is considerable interest in molecules with electrical properties that may be modulated by an external influence, for instance by electrostatic 'gating' from a third electrode,[8, 9] by irradiation with light,[10, 11] or by a chemical binding event.[12, 13] In the longer term, this will be important for molecular-scale devices or sensors. We have had a long-standing interest in the control of single molecule junction conductance using electrochemical gating.[14, 15] The use of a bipotentiostat and an electrolyte medium offers a way of overcoming the technical challenges inherent in fabricating a 3–terminal nanoscale device in which a molecule is in close enough proximity to the electrostatic gate to be switched by its electric field.[16] In strong electrolytes the Debye screening length can be extremely short, so although the counter and reference electrodes are physically far from the molecular bridge, any charge on the molecular bridge is screened by charge in solution at a distance much shorter than can usually be achieved in a solid state device. The result is a good and, significantly, a reproducible gate field. Using this approach, the junction conductances involving a structurally-diverse range of organic redox molecules (e.g. bis(thiaalkyl)viologens,[14, 17, 18] bis(thiahexyl)pyrrolotetrathiafulvalene (6PTTF6),[15, 17] oligoanilines[19, 20] and perylenetetracarboxylicdiimides[21, 22]) have been studied as a function of electrochemical

potential. Two distinct forms of behaviour were observed. In one case, the conductance changed monotonically as the redox process was traversed over a rather broad voltage range (denoted 'off-on' behaviour).[14, 21, 22] More rarely, the conductance rose to a peak value as the half-wave potential was approached, then fell again beyond it ('off-on-off' behaviour).[15, 17, 19] Attempts were made to model this theoretically, but it was not clear what factors were at work in determining the form of behaviour observed for a particular molecule or medium employed.[23, 24]

We, and others, have previously shown that ionic liquids (*e.g.* 1–butyl–3–methylimidazolium triflate orbis(trifluoromethyl-sulfonyl)imide salts, BMIM-OTf and BMIM-TFSI respectively) are useful media for single molecule conductance studies under potential control.[15] Their negligible vapour pressure makes them ideally suited for use with STM instrumentation and they have significantly wider potential windows than aqueous electrolytes. We have recently demonstrated that the conductance-potential behaviour observed for a small family of viologen redox molecules depends not upon the molecular structure, but rather, upon the degree of gate coupling mediated by the electrolyte, denoted in the well-known Kuznetsov-Ulstrup model by the gate coupling parameter ξ.[25] In aqueous electrolytes, the viologens displayed 'off-on' behaviour (as observed in earlier work[14, 17]) and ξ was 0.2, whereas in ionic liquids, they displayed 'off-on-off' behaviour and ξ was 1.

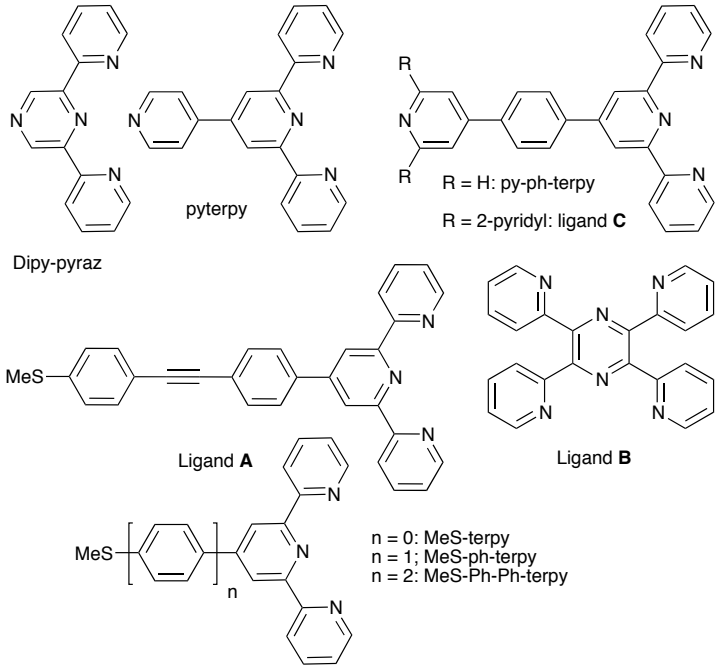

Scheme 1. Ligands discussed in this work.

Although the great majority of single molecule junction studies has to date involved organic molecules, the incorporation of metal centres into 'molecular wires' could offer significant potential advantages, for example in providing additional frontier orbital energies better-matched to the metal contact Fermi energies (in concert with reversible redox activity),[26, 27] or stable paramagnetic centres with a potential role in molecular spintronics.[28]. Two families of metal complexes in particular have often been put forward as candidates for molecular electronics (although actual metal | molecule | metal device studies on these systems remain sparse). The first is metal-alkynyl organometallic complexes, including multimetallic examples with bridging oligophenyleneethynylene (OPE) or oligocarbyne ligands.[29, 30] These could provide very long, rigid-rod molecules, readily functionalised with terminal contact groups and straightforward to characterise by NMR spectroscopy since they are diamagnetic.[31-33] Foci of interest with these molecules include comparison of their electrical properties with non-metal-containing OPE molecules to probe the influence of the metal(s),[34, 35] and the transition between tunnelling and hopping conductance mechanisms as a function of length.[36] The second family is derivatives of the ligand 2,2':6',2''-terpyridine (terpy), which have an extensive coordination chemistry; the ligand structure is amenable to

modification (for example to incorporate potential contact groups for junction formation), their metal complexes often have reversible redox activity and they can form relatively inert paramagnetic metal complexes amenable to junction formation experiments. For instance, oligomeric complexes of 'back-to-back' binucleating derivatives of terpy such as ligands **B** and **C** (Scheme 1) have been built up as monolayers on electrode surfaces by alternating reactions with excess ligand followed by excess metal ion (typically Co(II) or Fe(II)), and their redox behaviour has been characterised.[37-39] The electrical properties of some of these monolayers have been determined as a function of molecular length by using a macroscopic mercury electrode to make contact with the top of the monolayer. Remarkably low β values were claimed in this work, and these were metal–dependent (for Fe(II), 0.28 nm^{-1} and for Co(II), 0.01 nm^{-1}). This was ascribed to the operation of an intramolecular hopping mechanism.[37] *Single–molecule* conductance studies involving metal–terpy complexes are a very recent development,[27] although thiolated $[Co(terpy)_2]^{n+}$ derivatives were early subjects of a low–temperature Coulomb blockade and Kondo effect study using break junctions made by electromigration.[8] Using pre-synthesised mono- and dimetallic complexes of ruthenium(II), with combinations of ligands such as **A** (Scheme 1) and the back-to-back terpy derivative ligand **B** to afford thiomethyl-terminated complexes for junction formation, Davidson *et al*. found a β value of 1.5 nm^{-1} for this system, although unfortunately, synthetic limitations (ligand scrambling) precluded the selective syntheses of trimetallic or longer examples.[27]

Complexes of the ligand 4'-(pyridin-4-yl)-2,2':6',2''-terpyridine (pyterpy)[40] have been extensively used in supramolecular chemistry, for instance in polyheterometallic complexes in which octahedral $[M(pyterpy)_2]^{n+}$ complexes are coupled through subsequently-induced metal-pyridin-4-yl coordination,[41] in 'metalloviologen' compounds in which the pendant pyridine-4-yls are quaternised,[42] and in self-assembled monolayers where they are used to bind to a metal surface.[39] In this contribution, we report single molecule conductance studies on complexes $[M(pyterpy)_2]^{n+}$ (n = 2; M = Co, Fe, Ru: n = 3; M = Cr) and of some derivatives of pyterpy with varying molecular length, using the pendant pyridine-4-yl units as binding

sites for gold | terpyridyl complex | gold junctions. For $[M(pyterpy)_2]^{2+}$ (M = Co and Fe), we have examined the potential–dependent conductance of these complexes over their M^{II}/M^{III} redox waves in an ionic liquid medium. To test the effect of changing the binding group, we have also examined the length dependence of conductance for a related family of methylthioether-contacted terpy derivatives.

Results and Discussion

Synthesis and characterisation of the complexes

The ligand pyterpy[43] and its complexes $[M(pyterpy)_2](PF_6)_2$ (M = Co,[44] Fe[40] or Ru[45]) were synthesised by literature methods, or adaptations thereof. In addition, $[Co(pyterpy)_2](PF_6)_3$ was prepared by Br_2 oxidation of the Co(II) complex to allow characterisation by NMR spectroscopy. The complex $[Cr(pyterpy)_2](PF_6)_3$ was prepared from $CrCl_2$ and pyterpy, followed by metathesis with NH_4PF_6 and oxidation with $AgPF_6$, a method previously used to prepare $[Cr(terpy)_2](PF_6)_3$.[46] However, attempts to obtain a mass spectrum of this complex using the electrospray method failed, and we were unable to obtain microanalyses owing to the high percentage of fluorine in the complex. Characterisation was therefore restricted to a solution UV-visible spectrum, which showed similar charge transfer bands to those observed for $[Cr(terpy)_2]^{3+}$, and cyclic voltammetry; the complex showed a reversible 3+/2+ redox wave at –0.54 V *vs*. Fc/Fc^+ (CH_3CN/0.1 M Bu_4NBF_4), slightly anodic of the corresponding process for $[Cr(terpy)_2]^{2+/3+}$ at –0.63 V[46] as expected for the somewhat more electron-deficient ligand. The 'extended pyterpy' ligand 4'-(4-(pyridin-4-yl)phenyl)-2,2':6',2''-terpyridine (py-ph-terpy) was prepared by the route shown in Scheme 2; Suzuki coupling between 4-formylphenylboronic acid and 4-bromopyridine hydrochloride yielded 4-(pyridin-4-yl)benzaldehyde in 47 % yield. Subsequent reaction with two equivalents of 2-acetylpyridine followed in one pot by oxidative ring closure with ammonium acetate, afforded the target molecule in a yield of 34 %. This compound has previously been prepared in similar yield by Suzuki coupling of 4'-(4-bromophenyl)-2,2':6',2''-terpyridine with pyridin-4-ylboronic acid.[47]

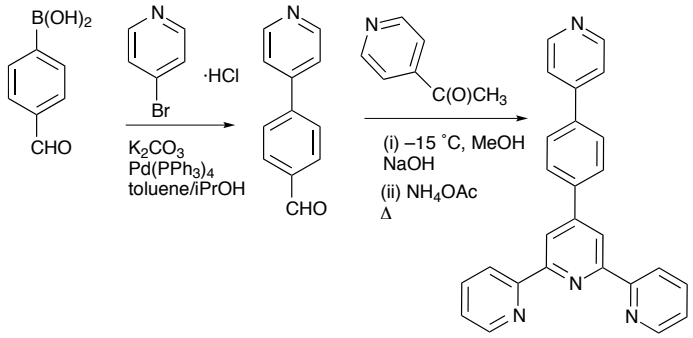

Scheme 2. Synthesis of py-ph-terpy

A shorter analogue of pyterpy, 2,6-di(pyridin-2-yl)pyrazine (dipy-pyraz; Scheme 1), was also prepared as described previously.[48] Ruthenium(II) complexes of dipy-pyraz and of py-ph-terpy, were prepared as hexafluorophosphate salts, from the ligand and '$RuCl_3 \cdot 3H_2O$' in hot ethylene glycol followed by metathesis with NH_4PF_6 (Experimental). Both the ligands and their Ru(II) complexes were characterized by ^{1}H NMR spectroscopy, electronic spectroscopy, microanalyses and mass spectrometry before single molecule junction experiments.

The ligands MeSterpy and MeS-ph-terpy (Scheme 1) were prepared using literature methods,[49, 50] as were their Ru(II) complexes (as hexafluorophosphate salts). [50] The new extended analogue 4'-(4'-(methylthio)-[1,1'-biphenyl]-4-yl)-2,2':6',2"-terpyridine (MeS-ph-ph-terpy) was prepared (albeit in low yield) by Suzuki coupling of 4'-(4-bromophenyl)-2,2':6',2''-terpyridine[51] with (4-(methylthio)phenyl)boronic acid. The corresponding Ru(II) complex $[Ru(MeS\text{-}ph\text{-}ph\text{-}terpy)_2](PF_6)_2$ was then prepared using the same conditions as for the other thiomethyl-terpy derivatives.

Single molecule junction conductance measurements in ambient conditions.

To measure the molecular junction conductances, we used the *I(s)* technique developed by Haiss *et al*.[4, 14] In this technique, contact between the Au STM tip and the surface is avoided. The tip is moved to a fixed distance above the Au substrate using the set point current, the feedback loop is disconnected and the tip is then retracted at constant speed while the tunnelling current I_s is monitored. Sub-monolayer coverages of molecules were previously

deposited on the substrates by briefly dipping them in dilute solutions of the appropriate molecule (see Experimental for details). The formation of a metal | molecule | metal junction is indicated by the presence in the current-distance ($I_s - s$) plot of a plateau. Pyridyl contact groups have been shown to result in multiple conductance values for the same molecule depending upon the precise experimental conditions used.[5, 52] In this work, we chose to use the conditions that we previously found to result in the lowest of the three conductance values seen for 4,4'-bipyridyl.[5] In brief preliminary experiments with 4,4'-bipyridyl as a model compound, the value found here (Table 1) was close to that found previously ($1.34 \pm 0.17 \times 10^{-4}\ G_0$).[5] The 'hit rate' (the proportion of *I-s* retraction experiments resulting in a plateau) was approximately 10 % with the set point current I_0 (40 nA) and bias V (0.6 V) used here.

Compound	**Conductance (G_0)**	**Expt. break-off (theoretical) (nm)**
4,4'-Bipyridine	$(1.0 \pm 0.3) \times 10^{-4}$	1.34 ± 0.24 (1.1)
$[Fe(pyterpy)_2](PF_6)_2$	$(4.4 \pm 1.3) \times 10^{-5}$	1.9 ± 0.3 (2.2)
$[Co(pyterpy)_2](PF_6)_2$	$(4.5 \pm 1.4) \times 10^{-5}$	1.95 ± 0.25 (2.2)
$[Cr(pyterpy)_2](PF_6)_2$	$(3.3 \pm 0.6) \times 10^{-5}$	1.92 ± 0.35 (2.2)
$[Ru(dipy\text{-}pyraz)_2](PF_6)_2$	$(8.6 \pm 1.9) \times 10^{-5}$	2.1 ± 0.4 (1.4)
$[Ru(pyterpy)_2](PF_6)_2$	$(4.8 \pm 1.2) \times 10^{-5}$	2.04 ± 0.27 (2.2)
$[Ru(py\text{-}ph\text{-}terpy)_2](PF_6)_2$	$(1.4 \pm 0.3) \times 10^{-5}$	3.0 ± 0.4 (3.1)
$[Ru(MeSterpy)_2](PF_6)_2$	$(9.6 \pm 2.3) \times 10^{-5}$	2.5 ± 0.5 (1.6)
$[Ru(MeS\text{-}ph\text{-}terpy)_2](PF_6)_2$	$(5.2 \pm 1.9) \times 10^{-5}$	2.2 ± 0.4 (2.4)
$[Ru(MeS\text{-}ph\text{-}ph\text{-}terpy)_2](PF_6)_2$	$(1.5 \pm 0.5) \times 10^{-5}$	3.2 ± 0.3 (3.3)

Table 1. Conductance values for all molecules measured in ambient conditions.

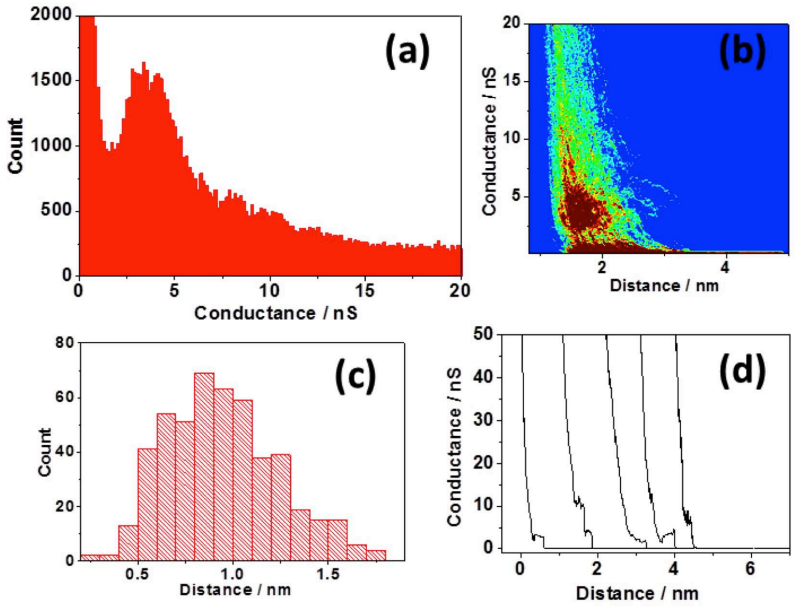

Figure 1. *I(s)* data recorded for $[Fe(pyterpy)_2](PF_6)_2$ in ambient conditions; I_0 = 40 nA, V_{bias} 0.6 V. (a) One-dimensional histogram of the 510 *I-z* traces collected that showed plateau(s), (b) two-dimensional representation of conductance *vs* corrected break-off distance for all plateau(s)-containing traces, (c) histogram of uncorrected break-off distances for all plateau(s)-containing traces, (d) some representative plateau(s)-containing *I-s* traces.

We then measured the conductances of junctions with each of the metal-pyterpy complexes, again measured in ambient with the same bias and I_0 as for 4,4'-bipyridine. Figure 1 shows a typical data set, that for $[Fe(pyterpy)_2](PF_6)_2$ (similar plots for the other complexes are presented in the SI). The hit rate for the complexes was somewhat lower than for 4,4'-bipyridine, approximately 5 %. The conductance values for $[M(pyterpy)_2](PF_6)_2$ (M = Fe, Ru and Co) are the same within experimental uncertainty, whereas the value for $[Cr(pyterpy)_2](PF_6)_3$ is somewhat lower (Table 1). Whereas both the Fe(II) and Ru(II) complexes are low–spin d^6, $[Co(pyterpy)_2]^{2+}$ is d^7 and, like some other Co(II)–terpy derivatives, it exhibits spin-crossover behaviour.[53] The Jahn-Teller-distorted, low-spin (^2E) state predominates at low temperature (110 K).[53, 54] The form of the temperature-dependent paramagnetism in the solid state is anion- and solvate-dependent; for the unsolvated PF_6 salt, 56 % of the complex is in the high-spin state at room temperature.[53] The Co(II)/Co(III) redox potential for this complex is – 0.04 V vs. Fc/Fc^+ (q.v.) and it is possible that on Au(111) in air, it becomes oxidised to Co(III); the Co(III) complex is also low–spin d^6, which would

mean that all three complexes in the conductance measurements are structurally– and electronically–similar, accounting for the similar conductance values. Attempts to determine the conductance of junctions starting with $[Co(pyterpy)_2](PF_6)_3$ were unsuccessful; it appears that this complex does not significantly adsorb on gold from those solvents in which it is soluble. It is interesting in this respect that the d^3 Cr(III) complex is the only example in this group with a significantly different junction conductance.

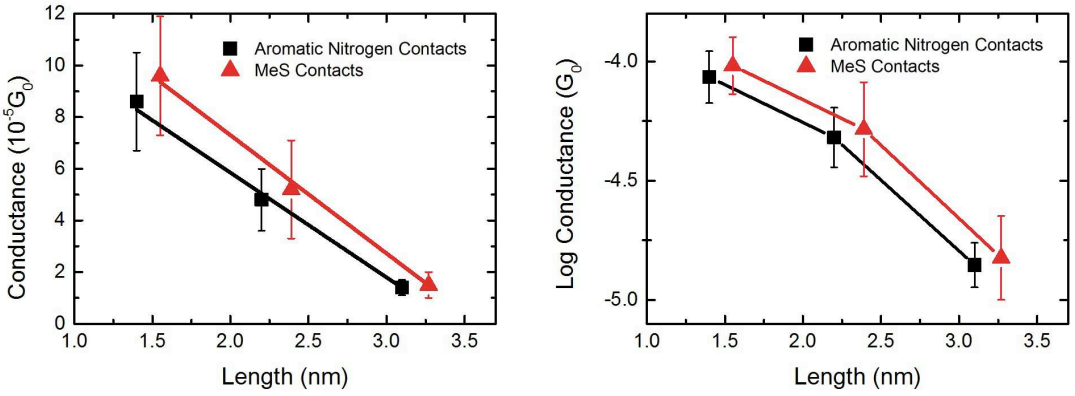

Figure 2 Conductance vs. length (left) and log(conductance) vs. length (right), for the ruthenium(II) complexes with aromatic nitrogen contacts, and with MeS contacts.

The conductances of the Ru(II) complexes with the pyterpy analogues, $[Ru(dipy\text{-}pyraz)_2]^{2+}$ and $[Ru(py\text{-}ph\text{-}terpy)_2]^{2+}$ were similarly determined in ambient (Table 1). The longest complex necessitated the use of a smaller I_0, 20 nA. Plots of conductance vs. molecular length and of log(conductance) *vs*. molecular length, with experimental uncertainties denoted as error bars, are shown in Figure 2. It should be noted that the plot of conductance *vs*. length is clearly linear, while the plot of log(conductance) *vs*. length deviates significantly from linearity. This may be preliminary evidence that a hopping-type mechanism is operating with these molecules, as suggested earlier for oligomeric metal complexes with 'back to back' terpy ligands.[37] A straight line of best fit for the log plot yields a β value of 1.06 nm^{-1}. This low β value can be compared with that previously found in STM break junction experiments, of 4.3 nm^{-1} for both amine- and carbon-contacted oligophenyls.[55] The fact that β is much smaller than that for the purely organic systems, in spite of the fact that in both cases the molecules are related by the successive extension of a polyphenylene-type chain, again

suggests a hopping-type mechanism may be operative for this series of ruthenium complexes.

To obtain more data on this issue, we extended the work to encompass a related series of thioether-contacted terpy derivatives (Scheme 1; Table 1), conveniently available by straightforward synthetic routes. The Ru(II) complexes of these ligands all gave good results in *I(s)* experiments under ambient conditions, producing a slightly higher hit rate (10-15 %) than the terpy-contacted molecules with otherwise identical experimental parameters. The conductance values are given in Table 1, and Figure 2 shows both linear and semi-log plots of conductance vs. molecular length. Again, it is clear that the linear fit is appreciably better than the semilogarithmic one, consistent with the notion of a hopping mechanism in this system. The linear best fit of the semilogarithmic plot gives a β value of 1.09 nm^{-1}, very similar to the value for the pyridyl–contacted series.

In all of these experiments, we also determined the mean break-off distances (the height *s* at which the junction breaks down), using a published method[56] (described in the supplementary information), and found that in most cases it was consistent with the full length of the molecules as calculated using molecular mechanics (Spartan14© version 1.1.8), implying that the conductance is characteristic of the fully extended molecules for this set of complexes. Very short molecules, such as 4,4'-bipyridine, $[Ru(dipy\text{-}pyraz)_2]^{2+}$ and $[Ru(MeSterpy)_2]^{2+}$ in this work, often give apparent break-off distances longer than the full molecular length with this method; this could be due to significant deviation from linearity in $d(\ln I)/d(s)$ at very short tip-sample separations in ambient.

Single molecule junction conductance measurements on $[M(pyterpy)_2](PF_6)_2$ (M = Co, Fe) under potential control.

We chose 1–(n-butyl)–3–methylimidazolium bis(trifluoromethylsulfonyl)imide (BMIM-TFSI) as the medium for studying the conductances of $[M(pyterpy)_2](PF_6)_2$ (M = Co, Fe) under electrochemical potential control. First, we examined the M(II)/M(III) redox waves of the complexes in BMIM-TFSI as a function of scan rate (Figure 3).

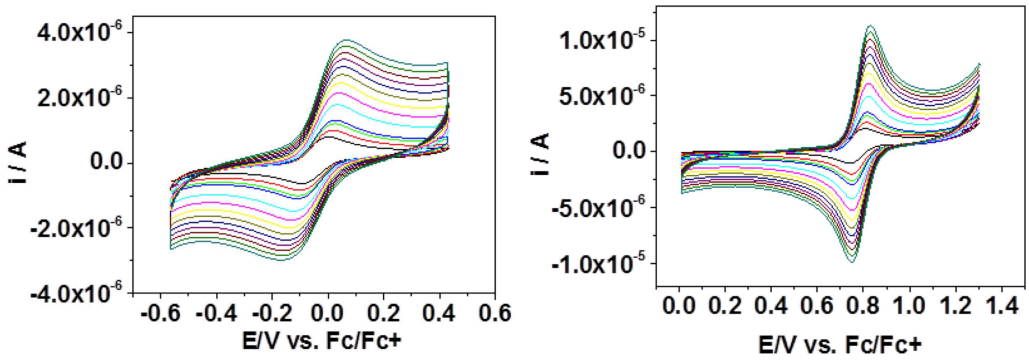

Figure 3 Cyclic voltammograms of (left) $[Co(pyterpy)_2](PF_6)_2$ and (right) $[Fe(pyterpy)_2](PF_6)_2$ in BMIM-TFSI, scan rates 0.02, 0.05, 0.08, then 0.1-1.0 V s^{-1} in 100 mV intervals.

The Fe(II)/Fe(III) process ($E_{1/2}$ = +0.78 V *vs*. Fc/Fc^+) is chemically reversible and the peak to peak separation increases only from 60 mV at 0.02 Vs^{-1} to 75 mV at 1.0 Vs^{-1}. The Co(II)/Co(III) process ($E_{1/2}$ = –0.04 V *vs*. Fc/Fc^+) is also chemically reversible, although clearly with slower electron transfer kinetics since the peak-to-peak separation increases from 80 mV at 0.02 Vs^{-1} to 240 mV at 1.0 Vs^{-1}. This is as expected since related low spin d^6/d^5 couples generally have small metal–ligand bond length differences and hence, low inner sphere reorganisation energies, while the d^7/low–spin d^6 process will involve a significant Co-N bond length change irrespective of whether the Co(II) state is high– or low–spin.[57]

Given the long timescale for collection of sufficient *I(s)* data to compile meaningful conductance histograms at many different electrode potentials, the fact that both redox forms are chemically stable on the experimental timescale in the ionic liquid, as demonstrated here, is important. *I*(*s*) data and corresponding conductance histograms were therefore collected for both complexes as a function of electrochemical potential across the M(II)/M(III) redox waves. The results are summarised in Figure 4 (histograms for individual experiments at each potential are presented in the SI). It is clear from the results that in ionic liquid electrolyte, both the Fe and Co complexes show 'off-on-off' behaviour, as observed earlier for 6PTTF6 in BMIM-TFSI across both of its redox waves (neutral/radical cation, and radical cation/dication),[15] and for viologens across the radical cation/dication redox wave.[25]

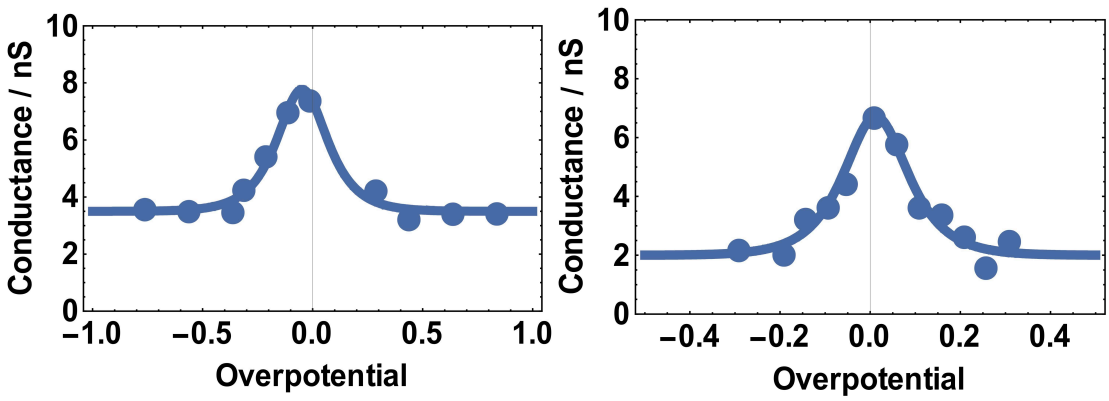

Figure 4. Conductance–overpotential plots for (a) $[Co(pyterpy)_2]^{2+/3+}$ and (b) $[Fe(pyterpy)_2]^{2+/3+}$ in BMIM TFSI. Data at each potential shown as points; the line corresponds to the fitting to the Kuznetsov-Ulstrup model, q.v.

As part of an earlier study of the relationship between molecular conductances and electrochemical rate constants for structurally-varied redox-active molecules, Zhou *et al.* studied the conductance of junctions of the complex $[Os(pyterpy)_2](PF_6)_2$ in aqueous 1 M $NaClO_4$ as a function of potential, using a technique very similar to the one employed here.[58] In their experiments, this complex showed 'on-off' conductance switching; the conductance changed sigmoidally from 23.1×10^{-5} G_0 (17.8 nS) in the Os(II) redox state to 2.70×10^{-5} G_0 (2.1 nS) in the Os(III) state. In contrast, we find that in the ionic liquid, the isoelectronic Fe complex switches from 2.70×10^{-5} G_0 (2.1 nS) in the 'off' state to *ca.* 8.4×10^{-5} G_0 (6.5 nS) in the 'on' state, then back to 2.70×10^{-5} G_0 (2.1 nS) as the complex is fully oxidised to Fe(III). Similarly, the Co complex switches from 4.5×10^{-5} G_0 (3.5 nS) in the 'off' state, to *ca.* 10.0×10^{-5} G_0 (7.7 nS) in the 'on' state, and back to 4.5×10^{-5} G_0 (3.5 nS) as the complex is fully oxidised to Co(III). This is similar to the situation for viologens, which show 'off-on-off' behaviour in ionic liquid but 'off-on' behaviour in aqueous electrolytes.

We have modelled the electrochemical single model conductance switching data for $[Co(pyterpy)_2]^{2+/3+}$ with the Kuznetsov Ulstrup 2-step charge transfer model. This model is illustrated in Figure 5. As shown in this figure the molecule bridges between the two

electrodes (the gold substrate surface and gold STM tip), with the metal redox centre tethered in the middle of this nano-gap. Hole transfer occurs through this redox centre in two electrochemical steps in what can be described as an electrochemical charge–hopping model. In this model the hole tunnels from the left electrode to the metal centre following pre-organisation of the molecule and its environment so that charge transfer can follow a Frank–Condon type transition. The molecule and its environment then relax, with the hole losing coherence during this relaxation. The hole then tunnels from the metal centre to right electrode. In the adiabatic limit, which is used here in the modelling, the relaxation prior to the second hole transfer step is partial. Following the first hole transfer the M(II) centre is oxidised and then subsequently reduced following charge transfer to other electrode. In the limit of strong electronic interactions between the redox centre and the electrodes the steady state current flow through the molecular junction is given by:

$$i = 2en\frac{k_1 k_2}{k_1 + k_2}$$

Where n represents the number of holes or electrons that can transfer in a "cascade" while the redox centre and its environment relaxes, and e is the electronic charge. k_1 and k_2 are electrochemical rate constant expressions.

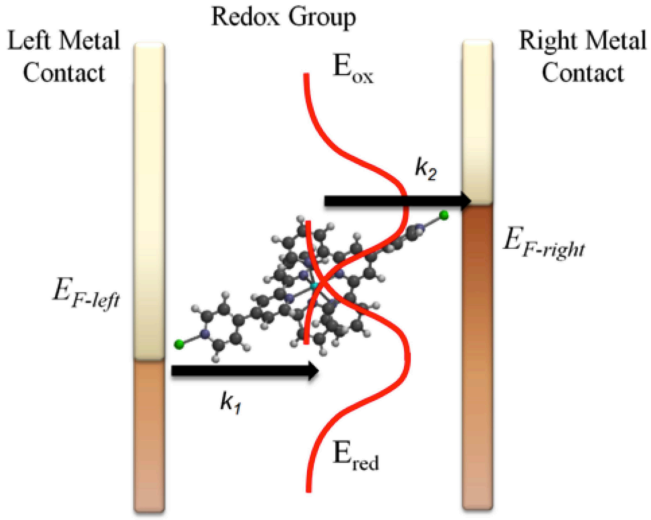

Figure 5. An illustration of the Kuznetsov Ulstrup model showing $[M(pyterpy)_2]^{2+/3+}$ attached between two gold electrode, labelled left and right respectively. The redox states of the molecule are illustrated in red with charge transfer occurring through these through two sequential electron transfer processes labelled k_1 and k_2.

Reference [59] describes the resulting equation which models the enhanced current following across the molecular junction (j_{enh}) following the two–step adiabatic model of Kuznetsov and Ulstrup described above.

$$j_{enh} \approx j_0 \exp\left(-\lambda/4k_BT\right) \frac{\exp\left(e|V_{bias}|/4k_BT\right)}{cosh\left(\frac{e(0.5-\gamma)V_{bias} - e\xi\eta}{2k_BT}\right)}$$

In this equation k_B is the Boltzmann constant, V_{bias} the bias voltage, T the temperature and e the charge on an electron. The overpotential is represented as η while γ is a modelling parameter representing the fraction of the bias voltage dropped at the redox site. The total reorganization energy is λ, which includes both inner and outer-sphere contributions. ξ The fraction of the electrochemical potential experienced at the redox site is ξ. An expression for the pre-factor, j_0, can be found in reference [59]:

$$j_0 = en\omega_{eff}/2\pi$$

with

$$n \approx eV_{bias}\left(\frac{1}{2\kappa_L\rho_L} + \frac{1}{\kappa_R\rho_R}\right)^{-1}$$

The additional terms here are as follows: κ is the electron transmission coefficient, ρ is the density of electronic states in the metal electrodes near the Fermi level and ω_{eff} is the effective nuclear vibrational frequencies. The subscripts L and R refer to the left and right electrodes, respectively. Using these equations a numerical form for the enhanced current flowing across the molecular junction (j_{enh}) can be obtained and single molecule conductance data vs. electrochemical potential can then be quantitatively analysed with respect to this model.

Figure 4 shows the results of such analyses for $[M(pyterpy)_2]^{2+/3+}$ (M = Fe, Co). The points in this plot show the experimental single molecule conductance data while the line is the fitting to the Kuznetsov Ulstrup 2-step model in the adiabatic limit. The fitting parameters for the cobalt complex are λ = 0.80 eV, ξ = 0.5 and γ = 0.40, while those for the iron complex are λ =

0.77 eV, ξ = 0.8 and γ = 0.55. The reorganization energies determined here are considerably less than previously found for a viologen single molecule bridge (1.3 eV) also determined in ionic liquid electrolytes.[25] The viologen single molecule bridge used in the latter work was called "6V6", where "V" refers to the viologen (bipyridinium) core which was attached to gold contacts at both ends through $-(CH_2)_6S-$ groups (donated here as "6"). The reorganisation energies of the pyterpy complexes obtained here are also considerably less than a similar analysis for both the first and second redox transitions for a 6PTTF6 bridge in ionic liquid environment, which gave values of λ = ~1.2 eV (6PTTF6 refers to the redox–active pyrrolo-tetrathiafulvalene (PTTF) moiety attached to gold contacts at both ends through $-(CH_2)_6S-$ groups). It is also noteworthy that in the 6V6 and 6PTTF6 examples ξ = ~1 was obtained. This value corresponds to the full electrochemical potential being experienced at the redox centre, indicative of the short Debye screening lengths of the ionic liquids and effective structuring of the ionic liquid in the nano-gap junction. In the case of the pyterpy studied here, ξ is lower indicating that the screening is not so effective. This may be due to the more "voluminous" redox centre with the metal ion redox centre being surrounded by a bulky ligand shell.

Conclusions

In a previous *I(s)* study of four related mono– and bi–metallic MeS–contacted Ru(II)-terpy complexes (including $[Ru(MeS\text{-}ph\text{-}terpy)_2]^{2+}$), it was found that a semilogarithmic plot of junction conductance vs. molecular length was approximately linear, with a decay constant β of 1.5 nm^{-1}, and a tunnelling mechanism was therefore suggested. However, these four molecules did not comprise a truly homologous series. In the present study, we have examined two homologous series, one with pyridyl and the other with MeS contacts, and both show a better fit of conductance vs. length than log(conductance) vs. length. Both also show a very low β for the semilogarithmic plots, of <1.1 nm^{-1}, whereas for a purely organic oligophenylene series, one would expect β to be 4.3 nm^{-1}.[55] This is evidence that a hopping-

type mechanism may be more appropriate for molecules of the type studied here. This is further supported by the observation that the conductance–overpotential relationships for the conductances of $[M(pyterpy)_2]^{2+/3+}$ under electrochemical potential control fit the Kuznetsov–Ulstrup relationship (essentially, a hopping-based description) so well.

A further examination of the conductances of junctions involving these molecules as a function of temperature may shed more light on the mechanism, although in this respect, it is worth noting that although we found evidence for a temperature dependence of the conductance of some oligoporphyrins, this could be accommodated within a tunnelling-based theoretical description, owing to relatively small thermal effects on the transmittance functions of these highly conjugated molecules having a significant effect upon their conductances.[60]

Experimental section

Synthesis and characterisation of ligands and complexes

Reagents were purchased from Sigma-Aldrich Chemical Company and used as received, except where otherwise stated. Proton and ^{13}C NMR spectra were recorder using a Bruker Avance 400 MHz spectrometer and were referenced to internal TMS. Mass spectra were recorded using a Carlo Erba 8000 Trio-1000 quadrupole spectrometer using electrospray, electron or chemical ionization, as appropriate. CHN microanalyses were recorded using an Isoprime Elemental Analyser (we were unable to record microanalytical data for samples containing >20 % fluorine with this analyser).

The ligand pyterpy[43] and its complexes $[M(pyterpy)_2](PF_6)_2$ (M = Co,[44] Fe[40] or Ru[45]) were synthesised by literature methods and the characterising data obtained was consistent with the literature. The ligands MeSterpy[49] and MeS-ph-terpy[50] and their Ru(II) complexes[50] were similarly prepared by literature methods or adaptations thereof.

Bis(4'-(pyridin-4-yl)-2,2':6',2''-terpyridine)chromium(III) hexafluorophosphate, [Cr(pyterpy)$_2$](PF$_6$)$_3$:- To degassed water (30 cm^3) was added 4'-(pyridin-4-yl)-2,2':6',2''-terpyridine (0.67 g, 2.19 mmol) and $CrCl_2$ (0.135 g, 1.10 mmol). The solution was stirred at room temperature for 20 h during which time the colour changed from light blue to dark brown. A degassed solution of aqueous NH_4PF_6 (5 mL; 0.44 M, 2.20 mmol) was added and a precipitate formed. The solid was filtered using a Schlenk stick, then washed with 50 cm^3 of degassed water, dried under vacuum, extracted with the minimum volume of dry CH_3CN (*ca*. 2 cm^3) and filtered. To this solution was added $AgPF_6$ (0.030 g, 0.12 mmol) in CH_3CN (1 cm^3) over 20 s with stirring. After 15 minutes the CH_3CN was removed under vacuum to afford a brown residue. The product was taken up in CH_3CN and filtered through Celite, and the solvent was removed under vacuum. The residue was triturated and then washed with THF, filtered and dried under vacuum to give the title compound as an orange solid (0.45 g, 37 %). UV/Vis (CH_3CN, 1.2 x 10^{-5} mol dm^{-3}) λ_{max}/nm ($\varepsilon_{max}/10^3$ dm^3 mol^{-1} cm^{-1}): 368 (21), 318 (sh), 282 (89.2). Cyclic voltammetry (0.1 M Bu_4NBF_4/CH_3CN): –0.54 V *vs.* Fc/Fc$^+$, reversible.

4'-(4-(pyridin-4-yl)phenyl)-2,2':6',2''-terpyridine (py-ph-terpy; see Scheme 2):- (a) 4-(Pyridin-4-yl)benzaldehyde– (This compound has previously been prepared in somewhat higher yield using a cyclopalladated species as catalyst[61]). (4-Formylphenyl)boronic acid (0.16 g, 1.06 mmol) and 2 M aqueous K_2CO_3 (2.6 cm^3) were added to a solution of 4-bromopyridine hydrochloride (0.2 g, 1.34 mmol) in toluene:*i*-PrOH (50:50, 4 cm^3). After degassing the solution for 15 mins using Ar, $Pd(PPh_3)_4$ (0.036 g, 0.030 mmol) was added and the mixture was refluxed for 7 h under Ar. After this time the reaction mixture was diluted with water and extracted with EtOAc. The combined organic layers were dried with $MgSO_4$ and the solvent was evaporated. Recrystallisation from EtOAc yielded the title compound as white needles (0.116 g, 47 %); m.p: 85-88 °C; ^{1}H NMR (400 MHz, $CDCl_3$): 10.11 (s, 1H, C*H*O), 8.75 (dd, *J* 4.6, 1.6 Hz, 2H), 8.03 (dd, *J* 6.8, 1.7 Hz, 2H), 7.83 (dd, *J* 6.8, 1.6 Hz, 2H), 7.65 (dd, *J* 4.65, 1.6 Hz, 2H); ^{13}C NMR (100 MHz, $CDCl_3$): 191.47 (*C*=O), 148.9, 147.0,

143.3, 136.8, 130.5, 127.9, 122.3; MS (CI^+ NH_3): m/z: 184.3. (b) *Reaction with 2-acetylpyridine*-A solution of 4-(pyridin-4-yl)benzaldehyde (0.05 g, 0.273 mmol) in methanol (4 mL) was cooled to –15°C. Solutions of 2-acetylpyridine (0.066 g, 0.54 mmol) in MeOH (2 mL) and 20 % aq NaOH (4 mL) were added simultaneously over a period of 20 minutes. The reaction mixture was then further stirred for 3 h at –10 °C then allowed to reach room temperature, and was filtered. The filtrate was treated with NH_4OAc (0.1 g, 1.297 mmol) and heated to reflux for 4 h. The resulting suspension was filtered and the solid washed several times with hot water and hot ethanol. The title compound was recovered as a white solid (0.036 g, 34 %); m.p: 220-225 °C. ^{1}H NMR (400 MHz, $CDCl_3$): 8.82 (s, 2H), 8.76 (s, 2H), 8.68 (m, 4H), 8.09 (d, *J* 8.3 Hz, 2H), 7.92 (td, *J* 7.7, 1.6 Hz, 2H), 7.84 (d, *J* 8.3 Hz, 2H), 7.75 (d, *J* 6.2 Hz, 2H), 7.41-7.38 (m, 2H). ^{13}C NMR (100 MHz, $CDCl_3$): 156.1, 156.0, 149.2, 149.1, 149.0, 139.6, 138.1, 137.0, 128.2, 127.6, 124.0, 121.9, 121.5, 118.8. MS (EI+): m/z: 386.5. UV/Vis (CH_3CN, 1.2 x 10^{-5} mol dm^{-3}) λ_{max}/nm ($\varepsilon_{max}/10^3$ dm^3 mol^{-1} cm^{-1}): 285 (209.4).

Bis(4'-(4-(pyridin-4-yl)phenyl)-2,2':6',2''-terpyridine)ruthenium(II) hexafluorophosphate, $[Ru(py\text{-}ph\text{-}terpy)_2](PF_6)_3$

A solution of '$RuCl_3{\cdot}3H_2O$' (0.019 g, 0.120 mmol) and 4'-(4-(pyridin-4-yl)phenyl)-2,2':6',2"-terpyridine (0.092 g, 0.240 mmol) in ethane-1,2-diol (10 cm^3) was heated to reflux for 3 h. The solution was allowed to cool, and water (10 cm^3) and an excess of methanolic NH_4PF_6 were added. The resulting dark brown precipitate was collected on Celite by filtration and then redissolved in CH_3CN. The CH_3CN was reduced to minimum volume *in vacuo*, and purification was by flash column chromatography (SiO_2, eluting with CH_3CN: sat. aq. KNO_3: water, 7:1:0.5). The first major orange fraction was collected, an excess of methanolic $NH_4[PF_6]$ was added, and the solution was evaporated to low volume to precipitate $[Ru(py\text{-}ph\text{-}terpy)_2](PF_6)_2$. The compound was filtered and dried in air to yield the title compound as a red solid (0.048 g, 46 %). ^{1}H NMR (CD_3CN), 400 MHz): 9.08 (s, 4H), 8.77 (dd, *J* 4.7, 1.5 Hz, 4H), 8.68 (d, *J* 7.95 Hz, 4H), 8.38 (d, *J* 8.45 Hz, 4H), 8.18 (d, *J* 8.45 Hz, 4H), 7.99-7.94 (m,

8H), 7.45 (d, *J* 5.5 Hz, 4H), 7.22-7.94 (m, 4H). MS (ES+, CH_3OH): m/z: 873 $[M\text{-}H\text{-}2PF_6]^+$, 1019 $[M\text{-}PF6]^+$. UV/Vis (CH_3CN, 1.2 x 10^{-5} mol dm^{-3}) λ_{max}/nm ($\varepsilon_{max}/10^3$ dm^3 mol^{-1} cm^{-1}): 493 (24.3), 310 (60.8), 287 (sh).

Bis(2,6-di(pyridin-2-yl)pyrazine)ruthenium(II) hexafluorophosphate, [Ru(dipy-pyraz)$_2$](PF$_6$)$_2$:- A solution of '$RuCl_3 \cdot 3H_2O$' (0.027 g, 0.105 mmol) and 2,6-di(pyridin-2-yl)pyrazine (0.05 g, 0.214 mmol) in ethane-1,2-diol (10 cm^3) was heated to reflux for 3 h. The solution was allowed to cool, and water (10 cm^3) and an excess of methanolic NH_4PF_6 were added. The resulting dark brown precipitate was collected on Celite by filtration and then extracted into CH_3CN. The CH_3CN was evaporated to minimum volume, and purification was by flash column chromatography (SiO_2, eluting with CH_3CN: sat. aq. KNO_3: water, 7:1:0.5). The first major orange fraction was collected, an excess of methanolic $NH_4[PF_6]$ was added, and the solution was reduced in volume to precipitate [Ru(2,6-di(pyridin-2-yl)pyrazine)$_2$][PF_6]$_2$. The compound was filtered and dried in air to yield the title compound as a red solid (0.04 g, 47 %). ^{1}H NMR (CD_3CN): 9.86 (s, 1H), 8.62 (d, *J* 8 Hz, 1H), 7.99 (td, *J* 8 Hz, 1.3 Hz, 1H), 7.36 (d, *J* 5.51 Hz, 1H), 7.20 (td, *J* 5.66, 1.13 Hz, 1H); ^{13}C NMR (100 MHz, CD_3CN): 153.76, 150.44, 144.39, 139.41, 128.56, 125.62; MS (ES+, CH_3OH): m/z: 569 $[M\text{-}H\text{-}2PF_6]$, 715 [M-PF6]; UV/Vis ($CH_3CN$, 1.2 x 10^{-5} mol dm^{-3}) λ_{max}/nm ($\varepsilon_{max}/10^3$ $dm^3mol^{-1}cm^{-1}$): 469 (9.5), 340 (sh), 308 (26.8), 269 (23.5).

4'-(4'-(methylthio)-[1,1'-biphenyl]-4-yl)-2,2':6',2''-terpyridine, MeS-ph-ph-terpy:- To a solution of 4'-(4-bromophenyl)-2,2':6',2''-terpyridine (0.23 g, 0.59 mmol) in toluene:*i*-PrOH (50:50, 4 cm^3) was added (4-(methylthio)phenyl)boronic acid (0.115 g, 0.61 mmol) and 2 M aqueous K_2CO_3 (2.6 cm^3). After degassing the solution for 15 mins with Ar, $Pd(PPh_3)_4$ (0.016 g, 0.014 mmol) was added and the mixture was refluxed for 7 h under Ar. After this time the reaction mixture was diluted with water and extracted several times with EtOAc. The combined organic layers were dried with $MgSO_4$ and the solvent was evaporated.

Recrystallisation from EtOAc yielded the title compound as white needles (0.025 g, 0.058 mmol, 10 %); m.p: 190-195 °C; ^{1}H NMR ($CDCl_3$), 400 MHz): 8.82 (s, 2H), 8.71 (m, *J* 7.7 Hz, 4H), 7.99 (d, *J* 8.3 Hz, 2H), 7.92 (t, *J* 7.7 Hz, 2H), 7.65 (d, *J* 8.3 Hz, 2H), 7.53 (d, *J* 8.4 Hz, 2H), 7.37 (t, *J* 5.6 Hz, 2H), 7.29 (d, *J* 8.4 Hz, 2H), 2.47 (s, 3H). ^{13}C{^{1}H} NMR (101 MHz, $CDCl_3$): 148.4, 141.3, 138.2, 137.0, 127.9, 127.4, 127.3, 127.0, 124.1, 121.9, 119.2, 14.8. MS (CI+ CH_4): m/z [M+H] 432; UV/Vis (CH_3CN, 9 x 10^{-6} mol dm^{-3}) λ_{max}/nm ($\varepsilon_{max}/10^3$ dm^3 mol^{-1} cm^{-1}): 279 (163.2).

Bis(4'-(methylthio)-2,2':6',2''-terpyridine)ruthenium(II) hexafluorophosphate, [Ru(MeSterpy)$_2$](PF$_6$)$_2$:- A solution of '$RuCl_3 \cdot 3H_2O$' (0.19 g, 1.20 mmol) and 4'-(methylthio)-2,2':6',2''- terpyridine (0.66 g, 2.4 mmol) in ethane-1,2-diol (100 cm^3) was heated at reflux for 12 h. The solution was allowed to cool, and water (10 cm^3) and an excess of methanolic NH_4PF_6 were added. The resulting dark brown precipitate was collected on Celite by filtration and then redissolved in CH_3CN. The CH_3CN was evaporated to minimum volume, and purification was by flash column chromatography (SiO_2, eluting with CH_3CN: sat. aq. KNO_3: water, 7:1:0.5). The first major orange fraction was collected, an excess of methanolic NH_4PF_6 were added, and the solution reduced in volume to precipitate [Ru(4'-(methylthio)-2,2':6',2''-terpyridine)$_2$][PF_6]$_2$. The compound was filtered and dried in air to yield the title compound as a red solid (0.21 g, 20 %). ^{1}H NMR (CD_3CN, 400 MHz): 8.54 (s, 4H), 8.50 (d, *J* 8.0 Hz, 4H), 7.90 (m, *J* 9.1, 1.3 Hz, 4H), 7.38 (d, *J* 5.0 Hz, 4H), 7.16-7.14 (m, 4H), 2.93 (s, SMe, 6H). ^{13}C{^{1}H} NMR (CD_3CN, 101 MHz): 158.4, 155.1, 153.1, 152.3, 138.4, 128.1, 125.0, 120.2, 14.8. MS (ES+, CH_3OH): *m/z*: 805.0 [M-PF_6]. UV/Vis (CH_3CN, 9 x 10^{-6} mol dm^{-3}) λ_{max}/nm ($\varepsilon_{max}/10^3$ dm^3 mol^{-1} cm^{-1}): 491 (11.2), 301 (sh), 281 (115.6). UV/Vis data are consistent with those for the chloride salt, prepared previously.[62]

Bis(4''-(4''-(methylthio)-[1,1''-biphenyl]-4-yl)-2,2':6',2''-terpyridine)ruthenium(II) hexafluorophosphate, [Ru(MeS-ph-ph-terpy)$_2$](PF$_6$)$_2$:- A solution of '$RuCl_3 \cdot 3H_2O$' (0.007g,

0.03 mmol) and 4'-(4'-(methylthio)-[1,1'- biphenyl]-4-yl)-2,2':6',2''-terpyridine (0.025 g, 0.06 mmol) in ethane-1,2-diol (2.5 cm^3) was heated to reflux for 3 h. The solution was allowed to cool, and water (2.5 cm^3) and an excess of methanolic $NH_4[PF_6]$ were added. The resulting dark brown precipitate was collected on Celite by filtration and then redissolved in CH_3CN. The CH_3CN was reduced to minimum volume, and purification was by flash column chromatography (SiO_2, eluting with CH_3CN: sat. aq. KNO_3: water, 7:1:0.5). The first major orange fraction was collected, an excess of methanolic $NH_4[PF_6]$ was added, and the solution was reduced in volume to precipitate $[Ru(MeS\text{-}ph\text{-}ph\text{-}terpy)_2](PF_6)_2$. The compound was filtered and dried in air to yield a red solid (0.012 g, 33 %). ^1H NMR (CD_3CN, 400 MHz): 9.07 (s, 4H), 8.68 (d, *J* 8.0 Hz, 3H), 8.34 (d, *J* 8.4 Hz, 3H), 8.10 (d, *J* 8.1 Hz, 4H), 8.03 (d, *J* 8.4 Hz, 4H), 7.96 (t, *J* 7.3 Hz, 6H), 7.85 (d, *J* 8.2 Hz, 4H), 7.45 (m, 4H), 7.19 (t, *J* 6.1 Hz, 4H), 2.76 (s, SCH_3, 6H). MS (ES+, CH_3OH): m/z: 995 ($M\text{-}HPF_6\text{-}PF_6$+MeOH), 1141 ($M\text{-}PF_6$+MeOH). UV/Vis ($CH_3CN$, 9 x 10^{-6} mol dm^{-3}) λ_{max}/nm ($\varepsilon_{max}/10^3$ $dm^3mol^{-1}cm^{-1}$): 494 (9.9), 311 (38.9), 287 (sh).

STM-based molecular junction conductances

First, molecules were adsorbed onto flame–annealed gold-on-glass samples from a 5×10^{-5} M CH_2Cl_2 solution of the appropriate complex. A freshly–cut Au STM tip was held above the surface at a fixed setpoint current (40 nA except for the longest molecules for which 20 nA was used) and bias voltage (+ 0.6 V) and then withdrawn at a speed of 40 nm s^{-1} while maintaining a constant *x*-*y* position. A current-vertical distance (*I*(*s*)) curve was collected during tip withdrawal. When molecular junction formation occurs, *I* decreases exponentially with *s* but is larger, at a given *s*, than in cases where no junction forms, and *I* typically then settles at a plateau value as *s* is increased, before abruptly decaying to zero on junction breakdown. Many such *I(s)* traces are recorded. Only those that contain plateaus (ca. 500 per data set) were collected together in histogram plots to determine junction conductance values. The occurrence of plateaus in many such *I*(*s*) curves results in peaks in the histograms. The

percentage of scans showing evidence of junction formation was usually in the range 5-10 % (ca. 15 % for the MeS–contacted molecules). Further details of data collection and processing, and of the procedure for estimating s_0, are in the electronic supplementary information.

Acknowledgements

We thank the EPSRC for funding (grants EP/C011511/1, EP/H035184/1 and EP/H015639/1).

References

1. J. P. Bergfield and M. A. Ratner, *Phys. Status Solidi B*, 2013, **250**, 2249–2266.
2. J. C. Cuevas and E. Scheer, *Molecular Electronics: An introduction to Theory and Experiment*, World Scientific, Singapore, 2010.
3. R. J. Nichols and S. J. Higgins, in *Ann. Rev. Anal. Chem.*, eds. R. G. Cooks and J. E. Pemberton, 2015, vol. 8, pp. 389-417.
4. R. J. Nichols, W. Haiss, S. J. Higgins, E. Leary, S. Martin and D. Bethell, *Phys. Chem. Chem. Phys.*, 2010, **12**, 2801-2815.
5. C. Wang, A. S. Batsanov, M. R. Bryce, S. Martin, R. J. Nichols, S. J. Higgins, V. M. Garcia-Suarez and C. J. Lambert, *J. Am. Chem. Soc.*, 2009, **131**, 15647-15654.
6. G. Sedghi, L. J. Esdaile, H. L. Anderson, S. Martin, D. Bethell, S. J. Higgins and R. J. Nichols, *Adv. Mater.*, 2012, **24**, 653-657.
7. V. Kolivoska, M. Valasek, M. Gal, R. Sokolova, J. Bulickova, L. Pospisil, G. Meszaros and M. Hromadova, *J. Phys. Chem. Letts.*, 2013, **4**, 589-595.
8. J. Park, A. N. Pasupathy, J. I. Goldsmith, C. Chang, Y. Yaish, J. R. Petta, M. Rinkoski, J. P. Sethna, H. D. Abruna, P. L. McEuen and D. C. Ralph, *Nature*, 2002, **417**, 722-725.
9. S. Kubatkin, A. Danilov, M. Hjort, J. Cornil, J.-L. Brédas, N. Stuhr-Hansen, P. Hedegård and T. Bjørnholm, *Nature*, 2003, **425**, 698-701.

10. S. Martin, W. Haiss, S. J. Higgins and R. J. Nichols, *Nano Lett.*, 2010, **10**, 2019-2023.

11. A. S. Kumar, T. Ye, T. Takami, B.-C. Yu, A. K. Flatt, J. M. Tour and P. S. Weiss, *Nano Lett.*, 2008, **8**, 1644-1648.

12. E. Leary, H. Hobenreich, S. J. Higgins, H. van Zalinge, W. Haiss, R. J. Nichols, C. M. Finch, I. Grace, C. J. Lambert, R. McGrath and J. Smerdon, *Phys. Rev. Lett.*, 2009, **102**, 086801 (4 pp).

13. A. Vezzoli, I. Grace, C. Brooke, K. Wang, C. J. Lambert, B. Xu, R. J. Nichols and S. J. Higgins, *Nanoscale*, 2015, **7**, 18949-18955.

14. W. Haiss, H. van Zalinge, S. J. Higgins, D. Bethell, H. Höbenreich, D. J. Schiffrin and R. J. Nichols, *J. Am. Chem. Soc.*, 2003, **125**, 15294-15295.

15. N. J. Kay, S. J. Higgins, J. O. Jeppesen, E. Leary, J. Lycoops, J. Ulstrup and R. J. Nichols, *J. Am. Chem. Soc.*,, 2012, **134**, 16817-16826.

16. M. Poot, E. Osorio, K. O'Neill, J. M. Thijssen, D. Vanmaekelbergh, C. A. van Walree, L. W. Jenneskens and H. S. J. van der Zant, *Nano Lett.*, 2006, **6**, 1031-1035.

17. E. Leary, S. J. Higgins, H. van Zalinge, W. Haiss, R. J. Nichols, S. Nygaard, J. O. Jeppesen and J. Ulstrup, *J. Am. Chem. Soc.*, 2008, **130**, 12204-12205.

18. Z. H. Li, I. Pobelov, B. Han, T. Wandlowski, A. Blaszczyk and M. Mayor, *Nanotechnology*, 2007, **18**, 044018.

19. F. Chen, J. JHe, C. Nuckolls, T. Roberts, J. E. Klare and S. Lindsay, *Nano Lett.*, 2005, **5**, 503-506.

20. J. He, F. Chen, S. Lindsay and C. Nuckolls, *Applied Physics Letters*, 2007, **90**.

21. X. Li, J. Hihath, F. Chen, T. Masuda, L. Zang and N. Tao, *J. Am. Chem. Soc.*, 2007, **129**, 11535-11542.

22. C. Li, V. Stepanenko, M.-J. Lin, W. Hong, F. Wuerthner and T. Wandlowski, *Phys. Stat. Sol. B*, 2013, **250**, 2458-2467.

23. J. Zhang, Q. Chi, A. M. Kuznetsov, A. G. Hansen, H. Wackerbarth, H. E. M. Christensen, J. E. T. Andersen and J. Ulstrup, *J. Phys. Chem. B*, 2002, **106**, 1131-1152.

24. W. Haiss, T. Albrecht, H. van Zalinge, S. J. Higgins, D. Bethell, H. Hobenreich, D. J. Schiffrin, R. J. Nichols, A. M. Kuznetsov, J. Zhang, Q. Chi and J. Ulstrup, *J. Phys. Chem. B*, 2007, **111**, 6703-6712.

25. H. M. Osorio, S. Catarelli, P. Cea, J. B. G. Gluyas, F. Hartl, S. J. Higgins, E. Leary, P. J. Low, S. Martin, R. J. Nichos, J. Tory, J. Ulstrup, A. Vezzoli, D. C. Milan and Q. Zeng, *J. Am. Chem. Soc.*, 2015, **137**, 14319-14328.

26. F. Lissel, F. Schwarz, O. Blacque, H. Riel, E. Loertscher, K. Venkatesan and H. Berke, *J. Am. Chem. Soc.*, 2014, **136**, 14560-14569.

27. R. Davidson, J.-H. Liang, D. C. Milan, B.-W. Mao, R. J. Nichols, S. J. Higgins, D. S. Yufit, A. Beeby and P. J. Low, *Inorg. Chem.*, 2015, **54**, 5487-5494.

28. A. C. Aragones, D. Aravena, J. I. Cerda, Z. Acis-Castillo, H. Li, J. Antonio Real, F. Sanz, J. Hihath, E. Ruiz and I. Diez-Perez, *Nano Lett.*, 2016, **16**, 218-226.

29. L. Luo, S. H. Choi and C. D. Frisbie, *Chem. Mater.*, 2011, **23**, 631-645.

30. S. Rigaut, *Dalton Trans.*, 2013, **42**, 15859-15863.

31. S. J. Higgins, R. Nichols, S. Martin, P. Cea, H. S. J. van der Zant, M. M. Richter and P. J. Low, *Organometallics*, 2011, **30**, 7-12.

32. G. Grelaud, N. Gauthier, Y. Luo, F. Paul, B. Fabre, F. Barriere, S. Ababou-Girard, T. Roisnel and M. G. Humphrey, *J. Phys. Chem. C*, 2014, **118**, 3680-3695.

33. A. Mulas, Y.-M. Hervault, L. Norel, S. Rigaut and C. Lagrost, *Chemelectrochem.*, 2015, **2**, 1799-1805.

34. L. Luo, A. Benameur, P. Brignou, S. H. Choi, S. Rigaut and C. D. Frisbie, *J. Phys. Chem. C*, 2011, **115**, 19955-19961.

35. S. Marques-Gonzalez, D. S. Yufit, J. A. K. Howard, S. Martin, H. M. Osorio, V. M. Garcia-Suarez, R. J. Nichols, S. J. Higgins, P. Cea and P. J. Low, *Dalton Trans.*, 2013, **42**, 338-341.

36. B. Kim, J. M. Beebe, C. Olivier, S. Rigaut, D. Touchard, J. G. Kushmerick, X. Y. Zhu and C. D. Frisbie, *J. Phys. Chem. C*, 2007, **111**, 7521-7526.

37. N. Tuccitto, V. Ferri, M. Cavazzini, S. Quici, G. Zhavnerko, A. Licciardello and M. A. Rampi, *Nature Mater.*, 2009, **8**, 41-46.

38. Y. Nishimori, K. Kanaizuka, T. Kurita, T. Nagatsu, Y. Segawa, F. Toshimitsu, S. Muratsugu, M. Utsuno, S. Kume, M. Murata and H. Nishihara, *Chem. Asian J.*, 2009, **4**, 1361-1367.

39. E. Figgemeier, L. Merz, B. A. Hermann, Y. C. Zimmermann, C. E. Housecroft, H. J. Guntherodt and E. C. Constable, *J. Phys. Chem. B*, 2003, **107**, 1157-1162.

40. E. C. Constable and A. Thompson, *J. Chem. Soc. Dalton Trans.*, 1992, 2947-2950. DOI: 10.1039/dt9920002947

41. S. S. Sun and A. J. Lees, *Inorg. Chem.*, 2001, **40**, 3154-3160.

42. E. C. Constable, C. E. Housecroft, M. Neuburger, D. Phillips, P. R. Raithby, E. Schofield, E. Sparr, D. A. Tocher, M. Zehnder and Y. Zimmermann, *J. Chem. Soc. Dalton Trans*, 2000, 2219-2228. DOI: 10.1039/b000940g.

43. L. Persaud and G. Barbiero, *Can. J. Chem. –Rev. Can. Chim.*, 1991, **69**, 315-321.

44. R. Indumathy, S. Radhika, M. Kanthimathi, T. Weyhermuller and B. U. Nair, *J. Inorg. Biochem.*, 2007, **101**, 434-443.

45. E. C. Constable and A. M. W. Cargill-Thompson, *J. Chem. Soc. Dalton Trans*, 1994, 1409-1418. DOI: 10.1039/dt9940001409.

46. C. C. Scarborough, K. M. Lancaster, S. DeBeer, T. Weyhermueller, S. Sproules and K. Wieghardt, *Inorg. Chem.*, 2012, **51**, 3718-3732.

47. W. Goodall, K. Wild, K. J. Arm and J. A. G. Williams, *J. Chem. Soc. Perkin Trans. 2*, 2002, 1669-1681. DOI: 10.1039/b205330f

48. L. J. K. Cook, F. Tuna and M. A. Halcrow, *Dalton Trans.*, 2013, **42**, 2254-2265.

49. K. T. Potts, P. Ralli, G. Theodoridis and P. Winslow, *Org. Synth.*, 1986, **64**, 189.

50. E. C. Constable, C. E. Housecroft, E. Medlycott, M. Neuburger, F. Reinders, S. Reymann and S. Schaffner, *Inorg. Chem. Comm.*, 2008, **11**, 518-520.

51. P. Korall, A. Borje, P. Norrby and B. Ákermark, *Acta Chem. Scand.*, 1997, **51**, 760-766.

52. S. Y. Quek, M. Kamenetska, M. L. Steigerwald, H. J. Choi, S. G. Louie, M. S. Hybertsen, J. B. Neaton and L. Venkataraman, *Nature Nanotech.*, 2009, **4**, 230-234.

53. X. Zhang, H. Xie, M. Ballesteros-Rivas, Z.-X. Wang and K. R. Dunbar, *J. Mater. Chem. C*, 2015, **3**, 9292-9298.

54. X. Zhang, Z.-X. Wang, H. Xie, M.-X. Li, T. J. Woods and K. R. Dunbar, *Chem. Sci.*, 2016, **7**, 1569-1574.

55. W. Chen, J. R. Widawsky, H. Vazquez, S. T. Schneebeli, M. S. Hybertsen, R. Breslow and L. Venkataraman, *J. Am. Chem. Soc.*, 2011, **133**, 17160-17163.

56. G. Sedghi, K. Sawada, L. J. Esdaile, M. Hoffmann, H. L. Anderson, D. Bethell, W. Haiss, S. J. Higgins and R. J. Nichols, *J. Am. Chem. Soc.*, 2008, **130**, 8582-8583.

57. N. Sutin, B. S. Brunschwig, C. Creutz and J. R. Winkler, *Pure Appl. Chem.*, 1988, **60**, 1817-1830.

58. X.-S. Zhou, L. Liu, P. Fortgang, A.-S. Lefevre, A. Serra-Muns, N. Raouafi, C. Amatore, B.-W. Mao, E. Maisonhaute and B. Schoellhorn, *J. Am. Chem. Soc.*, 2011, **133**, 7509-7516.

59. J. Zhang, A. M. Kuznetsov, I. G. Medvedev, Q. Chi, T. Albrecht, P. S. Jensen and J. Ulstrup, *Chem. Rev.*, 2008, **108**, 2737-2791.

60. G. Sedghi, V. M. Garcia-Suarez, L. J. Esdaile, H. L. Anderson, C. J. Lambert, S. Martin, D. Bethell, S. J. Higgins, M. Elliott, N. Bennett, J. E. Macdonald and R. J. Nichols, *Nature Nanotech.*, 2011, **6**, 517-523.

61. Z. C. Xiong, N. D. Wang, M. J. Dai, A. Li, J. H. Chen and Z. Yang, *Org. Lett.*, 2004, **6**, 3337-3340.

62. K. T. Potts, D. A. Usifer, A. Guadalupe and H. D. Abruña, *J. Am. Chem. Soc.*, 1987, **109**, 3961-3967.